# Simple Contagion Dynamics in Tree-like Networks*

Simon Board† and Moritz Meyer-ter-Vehn‡

July 29, 2024

**Abstract**

We characterize the effect of network structure on contagion dynamics in terms of simple ODEs that are asymptotically exact as the networks grow large. Undirected links and clustering slow the diffusion while re-matching of agents accelerates the diffusion. In regular networks the effects are small, less than one additional degree. In an application to strategic experimentation we trace out the implications for equilibrium experimentation and welfare.

## 1 Introduction

In the simple contagion model, also called the Susceptible-Infected (SI) model, agents infect their neighbors at Poisson rate. This is a workhorse model in epidemiology and the study of social networks (e.g. Jackson (2010, Chapter 7), Newman (2018, Chapter 16), Kiss et al. (2017)). Within economics, such models are often used to study the spread of information or behavior across society. For example, Kremer (1996) and Geoffard and Philipson (1996) use it to study agents' precautionary behavior in an epidemic. Bass (1969) and Campbell (2013) use it to study the awareness of a new product that spreads via word-of-mouth. And Banerjee (1993) and Board and Meyer-ter-Vehn (2024) study how Bayesian decision makers learn from one another.

This paper investigates how such contagion dynamics depend on network architecture. This question is important for positive reasons: In which networks would we expect rumors to propagate faster? It is also important for normative reasons: How can a policy maker

*We have received useful comments from Jeff Ely, PJ Lamberson, Mark Watson. Keywords: tree networks, experimentation, social learning. JEL codes: D83, D85. We gratefully acknowledge financial support from NSF Grant 2149291.

†UCLA, http://www.econ.ucla.edu/sboard/

‡UCLA, http://www.econ.ucla.edu/mtv/

speed up the knowledge of a new production process, or slow down the spread of an infectious disease? In particular, we consider a configuration model in which agents are connected via directed links (e.g. Twitter), undirected links (e.g. LinkedIn), or in triples (e.g. Facebook). These networks capture heterogeneity in links and clustering; for large populations, they are also "tree-like" making them highly tractable because neighbors' behavior is independent.

We have two main results. First, we characterize infection rates in our three networks via a one-dimensional ODE when the population is large. Second, we show that, for a fixed distribution of neighbors, infection rates are higher in directed networks than undirected ones, and higher in undirected networks than triangle ones. This result also shows that, for regular networks, the effect of network structure is small, bounded by one degree. For example, infection in an undirected network with $n$ neighbors is sandwiched between that in directed networks with $n$ and $n-1$ neighbors. We also characterize contagion with random matching and show that infection rates are sandwiched between that in directed networks with $n$ and $n+1$ neighbors. These results imply that network architecture is of second-order importance for dense networks (e.g. catching a cold) while they are critical in sparse networks (e.g. catching an STD).

Our SI results demonstrate the qualitative and quantitative importance of network structure in contagion models and provide a useful tool for economists. To demonstrate this, we apply our results to a model of experimentation on networks based on Board and Meyer-ter-Vehn (2024). In the model, agents exert effort experimenting with a new technology whose state is high or low. Agents learn from their own and neighbors' successes but do not observe neighbors' effort. In equilibrium agents experiment until an (endogenous) stopping time $\tau$, after which ideas spread via a contagion process. Parallel to our results on contagion processes, we rank equilibrium experimentation and welfare across the four types of networks and bound the effect of network structure by one degree.

Overall, our results provide a clean tool for analyzing the spread of behavior and information across networks. We believe they will be useful for other models where contagion is shaped by behavior and agents' incentives (e.g. behavioral epidemiology, spread of awareness of new products).

## 1.1 Literature

We draw from the rich mathematical epidemiology literature. The SI model is a standard workhorse in this literature and its contagion dynamics are studied in terms of differential equations both under random matching and for a fixed network, see Newman (2018, Chapter 16) and Kiss et al. (2017, Chapter 6.5). In particular, Miller (2011), following Volz (2008),

showed that contagion on an undirected tree can be characterize by a one-dimensional ODE. This was extended by Volz et al. (2011) who characterizes dynamics on a network with pairwise links and triangles using a higher-dimensional ODE.[1]

We extend this literature by solving for the contagion dynamics for directed and triangular networks in terms of one-dimensional ODEs, allowing us to derive sharp comparisons across these cases and with random matching models. Such comparisons are difficult since networks are high-dimensional and the status of agents becomes intertwined over times. For example, Kiss, Miller, and Simon (2017) write "A major challenge [...] is understanding the role of network clustering. [...] In part this is due to computational challenges when neighbors' statuses are correlated". Our key departure from the literature is that when an agent becomes infectious, she simultaneously infects all of her neighbors; in contrast, Volz et al. (2011) assumes that the links of an infected agent activate independently. This distinction is irrelevant in tree networks, but reduces the complexity under clustering. Another contribution of our paper is a simple yet rigorous proof, Proposition 1, that contagion dynamics in finite networks converge to those in infinite trees, assuming only finite expected degrees.[2]

In Section 3 we embed a "perfect good news" model of strategic experimentation with unobserved actions and private payoffs into a network. The underlying experimentation model is closely related to the observed action model of Keller, Rady, and Cripps (2005), the public payoff model of Bonatti and Hörner (2011), and the bad news model of Bonatti and Hörner (2017). Observational learning in networks was pioneered by Bala and Goyal (1998) who study myopic, non-Bayesian agents. The current model is based on Board and Meyer-ter-Vehn (2024), where we considered regular undirected random networks and compared welfare and aggregate learning as a function of density. The current paper studies different types of networks (directed, clustered) with nondegenerate degree distributions. We show that behavior on large random network converges to a tree (Proposition $1'$), a result we used in our prior paper, and compare behavior across networks (Proposition $2'$). For a more complete literature review see Board and Meyer-ter-Vehn (2024).

Many papers have tried to understand how network structure (e.g. clustering, random matching) affects contagion. Miller (2009) compares the percolation of the configuration model and an agent-based simulation with realistic clustering. Volz, Miller, Galvani, and Meyers (2011) derive analytical solutions for networks with clustering, and studies the effect

[1]The Volz equations have been extended in various directions. Ritchie, Berthouze, and Kiss (2016) adds general subgraphs to the network rather than just cliques.

[2]Decreusefond et al. (2012) and Janson, Luczak, and Winridge (2014) show related convergence results that use different proof techniques on different models. In particular, Decreusefond et al. (2012) shows convergence to a system of ODEs in the SIR model while Janson, Luczak, and Winridge (2014) considers a "repeated" variant of the configuration model. Our proof relies on our ability to characterize behavior using a one-dimensional ODE and allows us to make weaker assumptions on the degree distribution.

of clustering on dynamics numerically. In comparison to these papers, our one-dimensional ODEs allow us to get tight analytical comparisons across networks. The closest formal result is from Board and Meyer-ter-Vehn (2021) in which myopic agents sequentially choose to acquire information at a single point in time (as opposed to our experimentation model which features forward-looking agents who choose to acquire information at every point in time). The dynamics are characterized by an ODE but do not coincide with an SI process and, in contrast to Proposition 2′, our results did not speak to welfare.

# 2 Contagion

## 2.1 Model

**Networks.** We study simple contagion dynamics on three classes of configuration networks with $I \in \mathbb{N}$ nodes; anticipating the strategic model in Section 3 we refer to the nodes as "agents" $i, j, k, \ell...$ (Iris, John, Kata, Lili, ...). We study three types of random network $G \in \{\bar{G}, \vec{G}, \hat{G}\}$.

(a) *Undirected configuration model,* $\bar{G}$. Each agent draws a random iid number $N$ of "stubs", which we randomly connect into links $i \leftrightarrow j$. We then discard "self-links" between two stubs of the same agent $i$, "multi-links" between the same agent pair $i, j$, and the last left-over stub if the total number is odd.

(b) *Directed configuration model,* $\vec{G}$. Each agent draws a random iid number $N$ of "stubs", each of which consists of an "in-stub" (through which an agent can be infected) and an "out-stub" (through which the agent infects others). We then randomly connect in-stubs and out-stubs into directed links $i \to j$, and finally discard self- and multi-links.

(c) *Triangular configuration model,* $\hat{G}$. Assume $N$ is even. Each agent draws a random iid number $N/2$ of "stub-pairs", which we randomly connect into triangles $\{i, j, k\}$, discarding triangles that include self-links or multi-links.

**Notation.** In directed networks, we write $\mathcal{N}_i(G)$ for the agents connected to $i$'s in-stubs, and $\mathcal{N}_i^{-1}(G)$ for the agents connected to her out-stubs. In undirected and triangular networks $\mathcal{N}_i(G) = \mathcal{N}_i^{-1}(G)$. Write $N'$ for the degree distribution of $i$'s typical neighbor $j$ (including the backward link to $i$). All three of our networks exhibit the friendship paradox: As $I \to \infty$, the typical agent $i$ has $N$ neighbors, while the typical neighbor $j$ has $N'$ neighbors where,

$$\frac{\Pr(N' = n)}{\Pr(N' = m)} = \frac{\Pr(N = n)}{\Pr(N = m)} \frac{n}{m}.$$

Three commonly used examples are:

- Regular networks. The number of neighbors is degenerate, $N \equiv n$, and hence $N' = n$.
- Poisson networks. Inspired by Erdo-Renyi, $N \sim Pois(\lambda)$ and hence $N' = N + 1$.
- Pareto networks. To model super-spreaders, the epidemiology literature (e.g. Barthelemy et al. (2004)) often considers $\Pr(N = n) \propto n^{-\alpha}$, so $\Pr(N' = n) \propto n^{-(\alpha-1)}$.

We assume throughout that $E[N] < \infty$; in the experimentation model, we impose the stronger condition that $E[N'] < \infty$.[3] Write $\underline{N}$ for the minimal degree.

**SI Contagion Dynamics.** Time is continuous and infinite $t \in [0, \infty)$. At time $t = 0$, each agent is infected iid with probability $\epsilon \in (0, 1)$. Infected agents $i$ become infectious indepenently at rate 1, and then simultaneously spread to all neighbors $j \in \mathcal{N}_i^{-1}(G)$. Write $X_{i,t} = 1$ if agent $i$ is infected at time $t$, and otherwise $X_{i,t} = 0$. Denote $i$'s susceptibility by $S_{i,t} = 1 - X_{i,t}$. The process is a symmetric, time-homogeneous Markov chain, so we often drop the time and agent indices. We are particularly interested in the average infection rate: Denote $x = E[X_i] = \Pr[X_i = 1]$ and $s = E[S_i] = \Pr[S_i = 1]$ with $x_0 \equiv \epsilon > 0$, where expectations are taken over both the network $G$ and the contagion process $\{X_{i,t}\}$.

**Remarks.** The model of directed networks assumes that an agent's number of in-stubs equals the number of out-stubs. This means there is a friendship paradox, as in the undirected network, and enables the comparison across networks (Proposition 2). We discuss imperfect correlation in the conclusion.

The model of infection assumes that agent $i$ infects all of her neighbors at the same time. With undirected and directed networks, our results are unaffected if infections are independent across links. With triangle networks, it is important that when Iris infects her neighbor John she infects their joint neighbor Kata at the same time. With a disease, this might be because Kata spends time with John and Iris together, or because the infection goes from "dormant" to "active", at which point Iris infects her friends. With our experimentation model, it means that all of Iris's neighbors see when her experimentation succeeds. This assumption ensures that the infection rates of Iris's neighbors are independent conditional on her being susceptible and allows us to characterize behavior by a one-dimensional ODE. We discuss independent activation in Section 2.4.

We study clusters via triangles, but one can extend the results to clusters of any size, as in Volz, Miller, Galvani, and Meyers (2011). The key assumption is that there is only

[3]For example, with Pareto degrees, we have $E[N] < \infty$ iff $\alpha > 2$, and $E[N'] < \infty$ iff $\alpha > 3$.

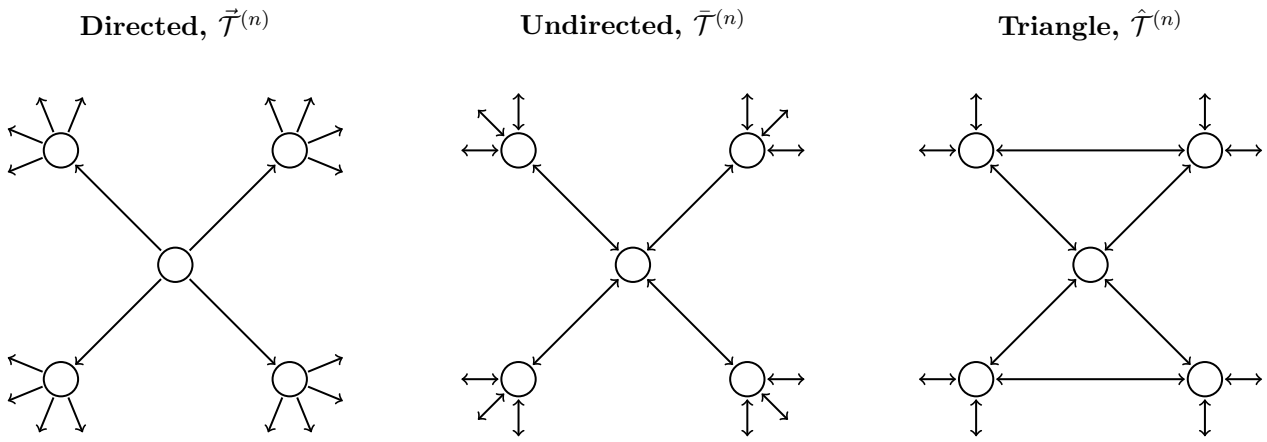


Figure 1: **Regular Trees** with degree $n = 4$.

one type of link; this allows us to charracterize dynamics via a one-dimensional ODE. We discuss how to extend our analysis to multiple types of links in Section 2.4.

## 2.2 Contagion Dynamics

In this section we describe contagion dynamic in large networks. Proposition 1, below, shows that, as $I \to \infty$, our network converges to a "tree network" of the following form, illustrated in Figure 1:

(a) Undirected network: A tree with $N$ neighbors, $N(N'-1)$ second neighbors, $N(N'-1)^2$ third neighbors,...

(b) Directed network: A tree with $N$ neighbors, $NN'$ second neighbors, $N(N')^2$ third neighbors,...

(c) Triangle network: A "triangle-tree" with $N$ neighbors, $N(N'-2)$ second neighbors, $N(N'-2)^2$ third neighbors,...

We now characterize infection rates in these three infinte tree networks. The key variable in our analysis is the probability that $i$'s neighbor $j$ is infected conditional on $i$ being susceptible[4]

$$a := E[X_j|S_i = 1] = 1 - \frac{E[S_j S_i]}{E[S_i]}. \tag{1}$$

The time-$t$ chance $j$ hasn't infected $i$ equals $e^{-\alpha_t}$ where $\alpha_t := \int_0^t a_u du$. To calculate the probability $i$ is susceptible, in the denominator of (1), note that $i$ is susceptible if she started

[4]Technically, the expectation fixes the agents $i, j$ and conditions the realization of the network $G$ on $j \in \mathcal{N}_i(G)$. Since the network is symmetric, $a$ does not depend on the identities of $i, j$.

susceptible and did not get infected by one of her $N$ neighbors. Since neighbors in a tree are independent,

$$s = E[S_i] = (1-\epsilon)E\left[\exp\left(-N\alpha\right)\right]. \tag{2}$$

The joint probability in the numerator of (1) depends on the kind of the network.

*Undirected network:* Neighbors $i$ and $j$ have $N_i+N_j-2 = N+N'-2$ additional neighbors (other than each other). In an infinite tree, each of these neighbors infects $i$ or $j$ with iid chance $\alpha$, so

$$E[S_jS_i] = (1-\epsilon)^2E\left[\exp\left(-(N_i+N_j-2)\alpha\right)\right]$$

Substituting back into (1) yields

$$a = 1-(1-\epsilon)E\left[\exp\left(-(N'-2)\alpha\right)\right]. \tag{3}$$

The "$-2$"-term adjusts for the double-counting of the link $i \leftrightarrow j$: Agent $j$ wastes one of his $N'$ stubs linking back to the susceptible $i$. The fact that conversely $i$ has not been infected by $j$ by time-$t$ further depresses the chance $j$ is infected.

*Directed network.* The only change in the analysis is that $i$ and $j$ have $N_i + N_j - 1$ additional neighbors, since $j$ does not waste a link on linking back to $i$. Thus

$$a = 1-(1-\epsilon)E\left[\exp\left(-(N'-1)\alpha\right)\right]. \tag{4}$$

*Triangle network.* Neighbors $i$ and $j$ share one common neighbor $k$ who, when infected, transmits to both of them at the same time. Thus, conditional on $i$ being susceptible, $S_j$ and $S_k$ are independent, and so $E[X_k|S_i = S_j = 1] = E[X_k|S_i = 1] = a$. Thus, $i$ and $j$ have $N_i + N_j - 3$ distinct neighbors (apart from each other and only counting $k$ once). Thus,

$$E[S_jS_i] = (1-\epsilon)^2E\left[\exp\left(-(N_i+N_j-3)\alpha\right)\right].$$

Substituting into (1) yields

$$a = 1-(1-\epsilon)E\left[\exp\left(-(N'-3)\alpha\right)\right] \tag{5}$$

Equations (2)-(5) tell us whether the infection will eventually reach all agents, $x_\infty := \lim x_t = 1$. In a directed network, everyone becomes infected iff they are all connected, $\underline{N} \geq 1$. In particular, (4) implies $a_t \geq \epsilon$ for all $t$, so $\alpha_t \geq \epsilon t$ and $\alpha_\infty = \infty$; since $\underline{N} \geq 1$ equation (2) then tells us $s_\infty = 0$. In an undirected network, (3) implies everyone becomes infected iff $\underline{N} \geq 2$. When $\underline{N} = 1$, the chance of connecting only to agents with a single link (which is wasted on linking back to $i$) upper-bounds $\alpha_t$ away from $\infty$, and $x_t$ from 1. In triangle networks, (5) implies everyone becomes infected iff $\underline{N} \geq 3$.

Equations (3)-(5) and their solutions $\{\bar{a}_t\}, \{\vec{a}_t\}, \{\hat{a}_t\}$ are exact in the associated infinite tree networks. Write $\{\bar{x}_t\}, \{\vec{x}_t\}, \{\hat{x}_t\}$ for the corresponding unconditional infection probabilities, derived from $x = 1 - s$ and (2). In finite, $I$-agent networks, $i$'s neighbors $j, k$ may be connected through paths avoiding $i$, and $i$'s neighbors are no longer independent. Let $a_t^I = E[X_j^I | S_i^I = 1]$ and $x_t^I = E[X_i^I]$ be the conditional and unconditional infection probabilities in a finite network, and write $\{\bar{a}_t^I\}, \{\vec{a}_t^I\}, \{\hat{a}_t^I\}, \{\bar{x}_t^I\}, \{\vec{x}_t^I\}, \{\hat{x}_t^I\}$ for these probabilities in our three kinds of configuration networks. We now show that, when $I$ is large, infection rates converge to those in the trees:

**Proposition 1.** *As $I \to \infty$, contagion dynamics in large random networks with degree $N$ converge to those in the respective infinite trees:*

(a) *Undirected networks: $\bar{a}_t^I \to \bar{a}_t$ and $\bar{x}_t^I \to \bar{x}_t$ for all $t$.*

(b) *Directed networks: $\vec{a}_t^I \to \vec{a}_t$ and $\vec{x}_t^I \to \vec{x}_t$ for all $t$.*

(c) *Triangle networks: $\hat{a}_t^I \to \hat{a}_t$ and $\hat{x}_t^I \to \hat{x}_t$ for all $t$.*

*Proof.* Focus on case (a). First, we show these random networks approximate trees as $I \to \infty$, by fixing a "root agent" $i$ and "uncovering the network" from this root. That is, we first randomly connect $i$'s link stubs, then the stubs of $i$'s $n$ neighbors, and so on. For fixed $n$ and $I \to \infty$, "$i$'s local network with radius $r \in \mathbb{N}$" $G_i^{I,r}$ is almost surely a tree. Second, we bound the effect of agents outside $G_i^{I,r}$ on $i$'s infection rates by ODEs that converge to (2) and (3) as $r \to \infty$. See Appendix A.2 for details. □

As a benchmark, we also consider contagion dynamics under *random matching* (with fixed, heterogeneous degrees $N_i$). To model this, assume that infected agents $i$ become infectious repeatedly (at rate 1). At such times $i$, infects $N_i$ other nodes, drawn randomly according to their degrees $N_j$ (independently across time). This model captures the idea that agents repeatedly interact with different people (e.g. infecting strangers on a plane).[5]

Write $a_n = a_{n,t}$ for the chance a degree-$n$ agent is infected by time-$t$, and $a = a_t = E[a_{N',t}]$ for the infection probability of a random neighbor. The agent is infected at time $t$ if she is susceptible and one of her $n$ neighbors infects her, $\dot{a}_n = n(1 - a_n)a$.[6] One readily verifies that this ODE-system is solved by $\tilde{a}_n := 1 - (1 - \epsilon)\exp(-n\tilde{\alpha})$ where $\tilde{a} = \dot{\tilde{\alpha}}$ solves the one-dimensional ODE

$$a = 1 - (1 - \epsilon)E[\exp(-N'\alpha)]. \tag{6}$$

[5]More generally, on a spectrum of time-varying networks $G_t$ that are randomly re-drawn at rate $\lambda$, random matching and fixed undirected networks are opposite extremes corresponding to $\lambda = \infty$ and $\lambda = 0$.

[6]This heuristic argument ignores correlation: the relevant rate of $j$ infecting $i$ is not $E[X_{j,t}]$, but $E[X_{j,t}|S_{i,t} = 1]$. Since neighbors are randomly redrawn, the effect of conditioning on $S_{i,t} = 1$ should vanish as $I \to \infty$. Niu (2002) proves convergence in a similar random matching model; with our focus on networks, we omit an adaptation of this proof to our random matching model.

We end with a literature note: Our approach follows the "edge-based compartmental model" introduced by Volz (2008) and Miller (2011) and surveyed in Kiss et al. (2017). Indeed, when removing the "recovery" state, equation (6.12a) in Kiss et al. collapses to our undirected dynamics (3).[7] Volz et al. (2011) study triangle nodes but, because infections happen independently across links, their dynamics do not reduce to one dimension, in comparison to (5). See Section 2.4 for details.

## 2.3 Comparative Statics

In this section, we examine the effect of network architecture and the degree distribution on contagion dynamics. Super-scripting infection rates with the degree distribution $x^{(N)}$ we have

**Proposition 2.** *For fixed degree distribution $N$, infection rates rank low-to-high: triangle networks, undirected networks, directed network, random matching*

$$\hat{x}_t^{(N)} < \bar{x}_t^{(N)} < \vec{x}_t^{(N)} < \tilde{x}_t^{(N)} \qquad \text{for all } t > 0. \tag{7}$$

*For regular networks, $N \equiv n$, the effect is less than one degree*

$$\hat{x}_t^{(n+3)} > \bar{x}_t^{(n+2)} > \vec{x}_t^{(n+1)} > \tilde{x}_t^{(n)} \qquad \text{for all } t > 0. \tag{8}$$

*Proof.* For fixed distribution $N$, the associated rankings for the neighbor's conditional infection rates $a$ follow immediately from the ODEs (3), (4), (5), and (6). These rankings translate to infection rates $x = 1 - s$ via (2). Intuitively, compared to the undirected tree, $i$'s infection rate is higher/lower in the directed/triangle tree since each neighbor $j$ has one additional/less second neighbor.

To see the converse cutoff-ranking (8) for regular networks, write the solutions to (3)-(6) as $\bar{\alpha}_t^{(N)}, \vec{\alpha}_t^{(N)}, \hat{\alpha}_t^{(N)}, \tilde{\alpha}_t^{(N)}$; neighbor's conditional infection rates differ by exactly one degree $\hat{\alpha}_t^{(n+3)} = \bar{\alpha}_t^{(n+2)} = \vec{\alpha}_t^{(n+1)} = \tilde{\alpha}_t^{(n)}$. Intuitively, each neighbor $j$ has $n+1$ second neighbors in each of the three trees. Unconditional infection rates $x = 1 - \exp(-n\alpha)$ additionally rise in

[7] To see this, drop the possibility of recovery, normalize the infection rate to 1 and set initial susceptibility to $1 - \epsilon$. Solving the dynamics at the level of $\theta = e^{-\alpha}$, the time-$t$ chance $j$ hasn't infected $i$, their equation (6.12a) becomes $\dot{\theta} = -\theta + (1-\epsilon)\frac{\hat{\psi}'(\theta)}{\hat{\psi}'(1)}$. Substituting the chance that $j$ has not been infected by his $N'-1$ forward-neighbors (other than $i$) $\frac{\hat{\psi}'(\theta)}{\hat{\psi}'(1)} = E[\theta^{N'-1}]$, we get $-\dot{\theta}/\theta = 1 - (1-\epsilon)E[\theta^{N'-2}]$, which is equivalent to (3).

Note that the heuristic approach in Newman's (2018, 16.5.2) yields a slightly different equation: Normalizing the infection rate to 1, setting initial susceptibility to $1-\epsilon$, equations (16.81) and (16.83) tells us that the law of motion of $a$ is given by (4) rather than (3) meaning the exponent is $(N'-1)$ rather than $(N'-2)$ since the approximation does not condition on $i$ not having been infected by $j$.

the number of first neighbors $n$ for given $\alpha$. $\square$

The first part of Proposition 2 provides a clean comparison of infection rates across networks. Random matching has the highest infection rate since Iris can be infected by $N'$ people at any point in time. In a directed network, Iris's chance of infection is lower since we know that her neighbor, John, didn't infected her in the past, lowering the probability that John is infectious. This captures the idea of how, during the Covid-19 pandemic, encouraging repeated interaction with the same people can lower infection. In an undirected network, infection is still lower since John cannot catch the infection from Iris. And infection is lowest in a triangle network since, if Iris is susceptible, then Kata cannot have infected John, further lowering John's infection rate. This captures the idea of how social pods further reduce the spread of Covid-19.

The second part of Proposition 2 quantifies the impact of network structure. It means that when agents have lots of neighbors (e.g. catching a cold from a colleague at work) link types are of second-order importance.[8] Conversely, network structure matters when the number of neighbors is small. For example, consider the spread of a sexually transmitted disease. In a monogamous society (a fixed undirected network with $N \equiv 1$) neighbor John's conditional infection rate vanishes $a_t \to 0$ by (3), and Iris's unconditional infection rate converges to the chance one of them starts out infected, $x_t \to 1-(1-\epsilon)^2 < 2\epsilon$. In contrast, when agents randomly interact with each other at the same rate (random matching with $N \equiv 1$) then both infection rates $a_t, x_t \to 1$ by (2) and (6).[9] Our finding that the importance of network architecture for dynamics falls with the degree echoes numerical findings by Melnik, Hackett, Porter, Mucha, and Gleeson (2011) who find that clustering is not very relevant for many real-world networks studies (e.g. University social networks constructed with Facebook data).

Next, we consider the effect of the degree distribution $N$. We focus on the case of undirected links. First, observe that an MLRP-rise in the number of neighbors raises infection rates $x$ and $a$; this follows immediately from equations (2) and (3). But it is less clear how other changes in the distribution, say, an increase in dispersion, affects contagion dynamics. To study this question we differentiate (3). Write $a_n := 1-(1-\epsilon)\exp(-(n-2)\alpha)$, so

[8]The proof of (8) assumes regular degrees but we believe the result to be more general. A key feature of regular networks is that when the degree $N$ rises by one, the neighbor's degree $N'$ also rises by one. In contrast, with other distributions $N'+1$ MLRP dominates $(N+1)'$, since $\frac{\Pr(N'+1=n)}{\Pr(N'+1=m)} = \frac{n-1}{m-1}\frac{\Pr(N+1=n)}{\Pr(N+1=m)} > \frac{n}{m}\frac{\Pr(N+1=n)}{\Pr(N+1=m)} = \frac{\Pr((N+1)'=n)}{\Pr((N+1)'=m)}$ for $n > m$. We thus get $\hat{\alpha}_t^{(N+3)} < \bar{\alpha}_t^{(N+2)} < \vec{\alpha}_t^{(N+1)} < \tilde{\alpha}_t^{(N)}$ and the ranking of $\hat{x}_t^{(N+3)}, \bar{x}_t^{(N+2)}, \vec{x}_t^{(N+1)}, \tilde{x}_t^{(N)}$ remains analytically ambiguous.

[9]One can similarly compare undirected and triangle networks. With $N \equiv 2$ neighbors, the undirected network is an infinite line with infection rates $a_t \equiv \epsilon$ and $x_t \to 1$, while the triangle network consists of disjoint triangles with $a_t \to 0$ and $x_t \to 1-(1-\epsilon)^3 < 3\epsilon$.

$E[a_{N'}] = a$ by (3). Then,

$$\frac{\dot{a}}{1-a} = \frac{E\left[(N'-2)(1-a_{N'})\right]a}{1-a} = \frac{E[(N'-2)\exp(-(N'-2)\alpha)]a}{E[\exp(-(N'-2)\alpha)]} = E[N_j - 2|S_i, S_j = 1]a. \tag{9}$$

For a regular network (9) reduces to $\dot{a} = (n-2)a(1-a)$. When $n = 2$ (the undirected line) Iris's conditional probability of infection from neighbor John is constant, $\dot{a} = 0$, as the good news from Iris not being infected by John is exactly offset by the chance John picks up an infection from his other neighbor Kata. When $n$ is higher, the conditional probability of infection increases over time as John can might pick up an infection from more than one agent. With non-degenerate degree distributions there is another effect: Iris's expectation of the number of John's neighbors falls over time. In particular, the likelihood ratio

$$\frac{\Pr(N_j = n|S_{i,t}, S_{j,t} = 1)}{\Pr(N_j = m|S_{i,t}, S_{j,t} = 1)} = \exp\left(-(n-m)\alpha_t\right) \tag{10}$$

reweights $N_j$ towards lower degrees as $j$ fails to infect $i$.[10] Similarly, unconditional infection rates $x$ follow

$$\frac{\dot{x}}{1-x} = E[N_i|S_i = 1]a. \tag{11}$$

Initially, a mean-preserving spread in the degree distribution raises contagion rates. To see this, note that for small $t > 0$ we can ignore the conditioning on $S_i, S_j = 1$ in (9) and (11), so infection rates $a$ are determined by the neighbor's expected degree $E[N'] = E[N^2]/E[N]$. A mean-preserving spread raises $E[N']$ and thereby infection rates $a$ and $x$. Indeed, for $E[N'] = \infty$ (9) implies $\dot{a}_0 = \infty$.[11] But eventually, a mean-preserving spread lowers infection rates. Recall the minimum degree $\underline{N}$.

**Proposition 3.** *Consider Networks 1 and 2 with degree distributions $(N_1, N_2)$ and initial infection rates $(\epsilon_1, \epsilon_2)$. If $\underline{N_1} > \underline{N_2}$ and $\underline{N_1} \geq 2$ then infection rates are eventually higher under Network 1, $x_t(N_1, \epsilon_1) > x_t(N_2, \epsilon_2)$ for all large enough $t$.*

*Proof.* See Appendix A.3. □

[10] The "$-2$"-term in (9), familiar from (3), implies that $a$ eventually falls if there's a chance that $N_j = 1$. Indeed, in that case $i$ is $j$'s only neighbor, and $j$ can only infect $i$ if he starts infected and the chance of that vanishes over time as $i$ remains uninfected.

[11] In the richer SIR model, where infected agents recover at a constant rate, this infinite slope of infection in networks with fat tails famously implies that the contagion can spread indepenently of the spreading rate (here normalized to one), skipping the exponential growth phase and immediately reaching a fixed proportion of the population; see e.g. Barthelemy, Barrat, Pastor-Satorras, and Vespignani (2004) for a heuristic derivation confirmed by numerical simulations for Pareto-degrees $\Pr(N = n) \propto n^{-\gamma}$ with tail-parameter $\gamma \in (2, 3]$. Analytically, we conjecture that $a_t$ is lower-bounded by some $\underline{a}_t > 0$ uniformly in the base rate $\epsilon > 0$.

Conditional on remaining susceptible, the expected number of neighbors of John and Iris in (9) and (11) fall over time, converging exponentially to $\underline{N}$ at rate $a$.[12] Once this expected degree is higher in Network 1, infection rates $a, x$ in Network 1 eventually overtake those in Network 2. Proposition 3 implies that contagion in a network with degree $N \sim U\{1, ..., 100\}$ eventually falls behind the simple line network, with $N \equiv 2$. Intuitively, with the uniform distribution, some agents are connected in pairs ($N = 1$) and are not reached by the infection; formally, as $E[N'] \to 1$, equation (9) turns negative and $a_t$ converges to zero. This argument relies on growth rates rather than levels and thus holds for any fixed base rates of infection $\epsilon_1, \epsilon_2 \in (0, 1)$.[13]

## 2.4 Discussion

The tight comparative static in Proposition 2 relies on various stark assumptions of our contagion model. But the approach of capturing contagion dynamics by small systems of ODEs that become exact as $I \to \infty$ extends far beyond. Here we sketch three such extensions.

**Correlated Base Rates.** Our model assumes that, at time-0, infection rates are IID. Given that the model captures degree-dependence and local correlation of infections at times $t > 0$, we can also allow some correlation at $t = 0$ without affecting our analysis. To be specific, assume that time-0 infections are degree-dependent $\epsilon_{N_i}$, with $\epsilon'_{N_j}$ for degree-$N_j$ neighbor $j$. We can also allow correlation of time-0 infections but assume that, conditional on $S_{i,0} = 1$, neighbors are asymptotically independent, $I \to \infty$. For example, the SI process may have been running prior to $t = 0$ and infected $i$ and her neighbors. The key assumption is that if an independent event infects Iris's neighbors John and Kata, it must also infect Iris. Contagion dynamics (2), (3) remain one-dimensional

$$s = E[(1 - \epsilon_N) \exp(-N\alpha)]$$
$$a = 1 - E[(1 - \epsilon'_{N'}) \exp(-(N' - 2)\alpha)].$$

**Independent Infections.** Our model assumes that an agent spreads the infection to all of her neighbors simultaneously. This captures "super spreader events" and is natural in our experimentation model. In contrast, Volz et al. (2011) assume that all infections

[12] The assumption $\underline{N} \geq 2$ guarantees the lower bound $a \geq \epsilon > 0$ that is necessary as well as sufficient for convergence to $\underline{N}$.

[13] This is not to say that base rates $(\epsilon_1, \epsilon_2)$ do not matter. If $\underline{N_1} = \underline{N_2}$ then the distribution of $(N_1, N_2)$ and the base rates $(\epsilon_1, \epsilon_2)$ both matter. Indeed, Proposition 3 has a converse: $x_t(N_1, \epsilon_1) > x_t(N_2, \epsilon_2)$ for large $t$ and all $(\epsilon_1, \epsilon_2)$ only if $\underline{N_1} > \underline{N_2}$ and $\underline{N_1} \geq 2$. Thus if $N_1 \equiv 2$ and $N_2 \sim U\{2, ..., 100\}$ then Network 1 can stay ahead if its base rate is high enough.

are independent of one another. Their assumption difference doesn't affect dynamics with binary links but does make the analysis of triangles more complicated: If $i, j, k$ form a triangle, and conditioning on $S_i = 1$, our correlation assumption ensures that $S_j$ and $S_k$ are independent, while (ironically) the standard independence assumption induces positive correlation between $S_j$ and $S_k$. To illustrate, consider a tree network with regular degrees $N \equiv n =: 2m$. Individual infection rates $s = E[S_i]$ still evolve as $\dot{s} = -2msa$ with neighbor's conditional infection rate $a = E[X_j|S_i = 1] = \frac{w+y}{s}$ computed from $w = E[S_i X_j X_k], y = E[S_i S_j X_k] = E[S_i X_j S_k]$, and $z = E[S_i S_j S_k]$, so $s = w + 2y + z$ and $a = \frac{w+y}{w+2y+z}$. Since neighbors outside the triangle $i, j, k$ infect at rate $a$ (pairs at rate $2a$), while infected triangle neighbors infect independently at rate 1, $w, y, z$ follow

$$\begin{aligned}
\dot{z} &= -6(m-1)za \\
\dot{y} &= 2(m-1)za - 4(m-1)ya - 2y \\
\dot{w} &= 4(m-1)ya + 2y - 2(m-1)wa - 2w
\end{aligned}$$

The contagion dynamics are thus governed by a three-dimensional system rather than a one-dimensional ODE.

**Heterogeneous Link Types.** Our model considers three simple networks (directed, undirected, triangle) as well as random matching. But, as in Volz et al. (2011), one might wish to have people connected via bilateral and triangle links to more closely match real-world networks. In our model, the dynamics of such a system are determined by a two-dimensional ODE. To see this, suppose agents draw independently $N$ "binary stubs" and $2M$ "triangle stub pairs", which randomly connect into binary links and triangles. Write Iris's unconditional infection rates as $x_t = E[X_{i,t}] = 1 - s_t$, and the neighbor's conditional infection rate as $a_t = 1 - E[X_{j,t}|S_{i,t} = 1]$ for binary neighbor John, and $b_t = 1 - E[X_{k,t}|S_{i,t} = 1]$ for triangle neighbor Kata, with cumulatives $\alpha$ and $\beta$. Then contagion dynamics are determined

$$\begin{aligned}
s &= (1-\epsilon)E[\exp(-N\alpha - 2M\beta)] \\
1 - a = \frac{E[S_i S_j]}{E[S_i]} &= (1-\epsilon)E[\exp(-(N'-2)\alpha - 2M\beta)] \\
1 - b = \frac{E[S_i S_k]}{E[S_i]} &= (1-\epsilon)E[\exp(-N\alpha - (2M'-3)\beta)]
\end{aligned}$$

which is a two-dimensional ODE. One could allow the number of binary and triangle stubs to be correlated; the resulting ODE would still be two-dimensional. Similarly, we could add types of agents to capture heterogeneous connection probabilities (i.e. a stochastic block model). When compared to Volz, Miller, Galvani, and Meyers (2011), our assumption of

correlated infections reduces the dimensionality of our ODE.

# 3 Experimentation

In this section we apply our contagion results to a simple model of experimentation on networks based on Board and Meyer-ter-Vehn (2024), henceforth BMtV24. That paper focused on the impact of density in regular networks, as they vary from sparse trees to dense cliques. Here we focus on tree networks and consider the effect of network architecture (directed, undirected, triangle, random matching) while allowing for non-degenerate degree distributions.

## 3.1 Model

**Networks.** As in Section 2.1, we study undirected, directed and triangle networks, $G = \bar{G}, \vec{G}, \hat{G}$ with $I \in \mathbb{N}$ agents $\{i, j, k, \ell ...\}$. The network describes whom agent $i$ observes. In particular, with a directed network, agent $i$ observes $\mathcal{N}_i(G)$ and is observed by $\mathcal{N}_i^{-1}(G)$. With undirected and triangle networks, $\mathcal{N}_i(G) = \mathcal{N}_i^{-1}(G)$.

**Game.** Each agent seeks to learn about the quality $\theta \in \{L, H\}$ of a new technology. At time $t = 0$, the common prior is $\Pr(\theta = H) = p_0$. At each time $t$, agent $i$ privately chooses effort $A_{i,t} \in [0, 1]$ at flow cost $c$. This effort results in successes with Poisson arrival rate $A_{i,t}\mathbb{I}_{\{\theta=H\}}$. Agent $i$ observes her own and her neighbors' past successes, but not others' actions. Agents perceive the network $G$ as random and independent of quality $\theta$.

**Payoffs.** Agents receive payoff $x > c$ from their own successes. Payoffs are discounted at rate $r > 0$, so Iris's net present value equals

$$V_i = \max_{\{A_{i,t}\}_{t\geq 0}} E\left[\int_0^\infty e^{-rt} A_{i,t}(x\mathbb{I}_{\{\theta=H\}} - c)dt\right] \tag{12}$$

where the expectation is taken over quality $\theta$, network $G$, and past observed successes on which $A_{i,t}$ conditions. We solve for weak perfect Bayesian equilibria, where agents who have observed a success infer that $\theta = H$. Since $x > c$, agents set $A_{i,t} \equiv 1$ after observing a success and obtain continuation value $y := (x - c)/r$. To avoid triviatilities we assume that the prior belief exceeds the *single-agent threshold belief*, $p_0 > \underline{p} := c/(x + y)$.

**Remark.** We assume that agent $i$ does not know the realization of her own degree $N_i$. Such uncertainty may capture applications where $N_i$ is the number of neighbors interested in adopting a new technology. This assumption simplifies our analysis by rendering equilibrium analyis one-dimensional, so simple monotonicty arguments guarantee a unique equilibrium. We extend our characterization of contagion dynamics to models of aymmetric information at the end of Section 3.3.

## 3.2 Preliminaries

We start of with two preliminary observations from BMtV24. We then explain how to map the model into into the SI contagion process from Section 2.

The first observation is that agents experiment until a symmetric cutoff time, $\tau$. BMtV24 (Proposition 1) shows that for any network and any strategies of others, agent $i$'s best response in the absence of observing a success is a cutoff strategy $\mathbb{I}_{\{t\leq\tau_i\}}$ for some cutoff $\tau_i \in [0,\bar{\tau}]$, where $\bar{\tau} = \log\frac{p_0(1-\underline{p})}{(1-p_0)\underline{p}}$. Moreover, since our configuration networks are exchangeable, BMtV24 (Corollary 1) shows there is a unique equilibrium and all agents use the same cutoff $\tau$. Thus, there is an *experimentation phase* until time $\tau$; in the high state $\theta = H$, some agents succeed, thereby seeding the network. After time $\tau$ there is a *contagion phase* as information diffuses across the network.

It is straightforward to characterize Iris's optimal cutoff as a function of her social learning. Conditioning throughout on $\theta = H$, she fails to succeed during her experimentation $[0,\tau]$ with probability $e^{-\tau}$. Conditional on not having succeeded herself, write $e^{-\beta_t}$ for her chance of not having observed a neighbor succeed either. Following BMtV24, we call $\beta = \{\beta_t\}$ the *social learning curve*. Iris's time-$t$ belief about quality then equals $p_t := \frac{p_0}{p_0+(1-p_0)e^{\min\{\tau,t\}+\beta_t}}$. The equilibrium threshold $\tau$ is given by the unique root of experimentation incentives

$$\psi_\tau(\beta) = p_\tau\left(x + ry\int_\tau^\infty e^{-r(t-\tau)-(\beta_t-\beta_\tau)}dt\right) - c. \tag{13}$$

When there is no social learning, $\beta_t = 0$, the integral simplifies to $1/r$ and the stopping belief $p_\tau$ coincides with the single-agent threshold $\underline{p} := c/(x+y)$. As social learning $\{\beta_t\}$ increases, $p_\tau$ falls as social learning crowds out private experimentation.[14] As social learning explodes, the integral vanishes, and $p_\tau$ converges to the myopic threshold $\overline{p} := c/x$.

The second observation is that equilibrium welfare can be expressed as function of the stopping time and the pre-cutoff social learning $\mathcal{V}(\tau,\beta_\tau)$. In particular, BMtV24 (Lemma 2) shows that this function takes the form:

[14] To see this, note that $\psi$ falls in $\beta = \{\beta_t\}_{t\geq 0}$ and single-crosses from above in $\tau$, so the root $\tau$ of $\psi_\tau(\beta)$ falls in $\beta$.

$$\mathcal{V}(\tau, \beta_\tau) = \frac{p_0 x - c}{r} + e^{-r\tau}\left(p_0 e^{-\beta_\tau - \tau}(x-c) - (1-p_0)c\frac{r-1}{r}\right) \tag{14}$$

and that $\partial_\tau \mathcal{V} < \partial_\beta \mathcal{V} < 0$. This fact that values fall in social information sounds surprising; it arises because we are fixing the stopping time, which is an endogenous function of social learning. As we will see, this result is useful to compare equilibrium welfare across agents and networks since $\tau$ and $\beta_\tau = -\log E[e^{-N\tau}]$ are easily characterized in equilibrium.

We now map the equilibrium behavior of the experimentation model to the SI contagion model of Section 2. We say that Iris is "infected" if she has observed a success, either by herself or by some neighbor $j \in \mathcal{N}_i(G)$, and otherwise "susceptible". The initial experimentation phase $t \in [0, \tau]$ determines the base rate $x = 1 - e^{-(N_i+1)\tau}$. In the contagion phase $t \in [\tau, \infty)$, infected agents spread to their susceptible neighbors at rate 1 (simultaneously across neighbors). As in Section 2.4, infections correlate across agents with degree-dependent rates already at the start of the contagion $t = \tau$ and the dynamics remain highly analogous.

## 3.3 Results

In this Section we characterize behavior on trees, show that this describes behavior on large configuration networks, and then compare stopping times and values across networks. As in Section 2.2, we analyze the experimentation rates of $i$'s neighbor $j$, $a_t = E[A_{j,t}|S_{i,t} = 1]$ in trees. During the experimentation phase $t \in [0, \tau]$, clearly $a_t \equiv 1$. During the contagion phase $t \in [\tau, \infty)$, $j$ experiments iff she has been infected by observing a success, so

$$a_t = 1 - E[S_{j,t}|S_{i,t} = 1] = 1 - \frac{E[S_{i,t}S_{j,t}]}{E[S_{i,t}]}$$

as in equation (1). The denominator is $s_t = E[S_{i,t}] = E\left[\exp(-\tau - N\alpha_t)\right]$, where $\alpha_t = \int_0^t a_u du$.

Adapting equations (3)–(5) for the period of initial experimentation, we can characterize learning in our networks. In the *undirected network,* the pair $(i, j)$ have $N + N' - 2$ independent neighbors which yields,

$$1 - a_t = \frac{E\left[\exp(-2\tau - (N + N' - 2)\alpha_t)\right]}{E\left[\exp(-\tau - N\alpha_t)\right]} = E\left[\exp(-\tau - (N' - 2)\alpha_t)\right], \tag{15}$$

with base rate $a_\tau = 1 - E[\exp(-(N' - 1)\tau)]$, capturing both the dependence on neighbor John's degree $N'$ and the correlation accross neighbors, with the "$-1$" accounting for Iris remaining susceptible.[15]

[15]For a stark instance of the effect of time-$\tau$ correlation, consider a network of dyads, $N \equiv 1$. Neighbors $i, j$ are either infected during experimentation $t \in [0, \tau]$ or never, as captured by $a_\tau = 0$.

In the *directed network,* the pair $(i, j)$ have $N + N' - 1$ independent neighbors since $j$ does not observe $i$,

$$1 - a_t = E\left[\exp(-\tau - (N' - 1)\alpha_t)\right]. \tag{16}$$

In the *triangle network,* the pair $(i, j)$ have $N + N' - 3$ independent neighbors since they share some neighbor $k$,

$$1 - a_t = E\left[\exp(-\tau - (N' - 3)\alpha_t)\right]. \tag{17}$$

Let $\bar{\alpha}_t, \vec{\alpha}_t, \hat{\alpha}_t$ be the solutions of (15)-(17) and denote the associated learning curves $\bar{\beta}_t, \vec{\beta}_t, \hat{\beta}_t$ as defined $\beta_t = E[\exp(-N\alpha_t)]$.

**Lemma 1.** *Assume $E[N'] < \infty$. There exist unique equilibrium thresholds $\bar{\tau}, \vec{\tau}, \hat{\tau}$ that solve $\psi_\tau(\beta) = 0$ for the associated social learning curves $\bar{\beta}_t, \vec{\beta}_t, \hat{\beta}_t$.*

*Proof.* Uniqueness follows since $\beta$ rises in $\tau$ and $\psi$ falls in $\beta$ and single-crosses from above in $\tau$. Existence relies on the continuity of $\beta_t$ as a function of $\tau$, as established in the proof of Proposition 2′.[16] □

We now show that stopping times and learning curves in large, finite configuration networks converge to those in trees. For fixed cutoff $\tau$, these heuristic equations are exactly correct in infinite tree networks and Proposition 1 shows that they approximate the contagion dynamics of large random networks. In Proposition 1′ the cutoff adjusts endogenously in equilibrium. Write $\bar{\tau}^I, \vec{\tau}^I, \hat{\tau}^I$ and $\bar{\beta}^I, \vec{\beta}^I, \hat{\beta}^I$ for equilibrium cutoffs and social learning curves in the finite networks.

**Proposition 1′.** *Assume $E[N'] < \infty$. The equilibria of the large random networks with degree $N$ converge to the equilibria of the respective infinite $N$-trees:*

(a) *Undirected networks: $\bar{\tau}^I \to \bar{\tau}$ and $\bar{\beta}^I_t \to \bar{\beta}_t$ for all $t$.*

(b) *Directed networks: $\vec{\tau}^I \to \vec{\tau}$ and $\vec{\beta}^I_t \to \vec{\beta}_t$ for all $t$.*

(c) *Triangle networks: $\hat{\tau}^I \to \hat{\tau}$ and $\hat{\beta}^I_t \to \hat{\beta}_t$ for all $t$.*

*Proof.* See Appendix A.2. □

Analogously, with *random matching,* we can adapt equation (6). Since there is no inference from the lack of past success that occurs in a fixed network, we have

$$1 - a_t = E\left[\exp(-\tau - N'\alpha_t)\right]. \tag{18}$$

[16] Continuity fails at $\tau = 0$ when $E[N'] = \infty$, and equilibrium may fail to exist in this case. For $\tau = 0$, we clearly have $\beta_t \equiv 0$, but the exploding number of second neighbors lower-bounds $\beta_t$ away from 0 for fixed $t > 0$ and any $\tau > 0$, as in footnote 11.

Let $\tilde{\alpha}_t$ be the solution and $\tilde{\beta}_t$ be the social learning curve. By Lemma 1, there is a unique threshold $\tilde{\tau}$ that solves $\psi_\tau(\beta) = 0$.

We can now rank cutoffs and values across networks. Superscripting equilibrium cutoffs and values with the degree $N$, we get

$$\hat{x}_t^{(N)} < \bar{x}_t^{(N)} < \vec{x}_t^{(N)} < \tilde{x}_t^{(N)} \qquad \text{for all } t > 0. \tag{19}$$

For regular networks, $N \equiv n$, the effect is less than one degree

**Proposition 2′.** *Assume $E[N'] < \infty$. For fixed degree distribution $N$, equilibrium cutoffs rates rank low-to-high: random matching, directed networks, undirected networks, triangle networks; values rank in the opposite way*

$$\tilde{\tau}^{(N)} < \vec{\tau}^{(N)} < \bar{\tau}^{(N)} < \hat{\tau}^{(N)} \qquad \tilde{V}^{(N)} > \vec{V}^{(N)} > \bar{V}^{(N)} > \hat{V}^{(N)}. \tag{20}$$

*For regular networks, $N \equiv n$, the effect is less than a degree*

$$\hat{\tau}^{(n+3)} < \bar{\tau}^{(n+2)} < \vec{\tau}^{(n+1)} < \tilde{\tau}^{(n)} \qquad \hat{V}^{(n+3)} > \bar{V}^{(n+2)} > \vec{V}^{(n+1)} > \tilde{V}^{(n)} \tag{21}$$

*Proof.* To see the cutoff-ranking in (20), note that for identical cutoffs $\tau$ the ODEs (15)-(18) imply $\tilde{\alpha}^{(N)} > \vec{\alpha}^{(N)} > \bar{\alpha}^{(N)} > \hat{\alpha}^{(N)}$. Since $\alpha$ rises in $\tau$, $\beta$ rises in $\alpha$, and $\psi_\tau(\beta)$ falls in $\beta$ and single-crosses from above in $\tau$, the equilibrium cutoffs must rank oppositely to ensure equilibrium, $\psi_\tau(\beta) = 0$. The value-ranking in (20) follows from the cutoff-ranking since pre-cutoff social learning $\beta_\tau = -\log E[\exp(-N\tau)]$ rises in $\tau$ and $N$, and $\mathcal{V}(\tau, \beta_\tau)$ falls in $(\tau, \beta_\tau)$.

To see the converse cutoff-ranking in (21) for regular networks, recall from the proof of Proposition 2 that for fixed $\tau$ the difference in degrees exactly undoes the difference in cofficients in (15)-(17), so $\hat{\alpha}^{(n+3)} = \bar{\alpha}^{(n+2)} = \vec{\alpha}^{(n+1)} = \tilde{\alpha}^{(n)}$. But since aggregate social learning $\beta_t = n\alpha_t$ rises in $n$ additionally via the number of first neighbors, fixed cutoffs imply $\hat{\beta}^{(n+3)} > \bar{\beta}^{(n+2)} > \vec{\beta}^{(n+1)} > \tilde{\beta}^{(n)}$, so equilibrium cutoffs adjust as in (21). Comparing equilibrium cutoffs is the hardest part of the proof since cutoffs adjust; Appendix A.4 shows that this doesn't overwhelm the ranking in social welfare. □

Proposition 2′ shows that cutoffs and values in, say, a triangle network with $n$ neighbors is sandwiched between that in a undirected network with $n$ and $n-1$ neighbors. This result is important for two reasons. First, it provides comparative statics across canonical networks in terms of experimentation, social learning, and welfare. In contrast, the rest of the literature typically focuses on long run considerations (e.g. whether the agents reach consensus or aggregate information). Second, it allows us to quantify the importance of

clustering, directed links, and fixed networks in the discovery and diffusion of ideas. This matters for network design (e.g. reducing clustering is useful, but adding connections is even better). It can also be useful for empirical work since we need not worry about exactly specifying the network (at least, within a class) if agents have many neighbors; this allows us to employ well understood models such as dyadic link formation networks (e.g. Graham, 2017).

Now consider the effect of the degree distribution $N$ on equilibrium experimentation and welfare. It is easy to see that the equilibrium cutoff $\tau$ falls in $N$: $\alpha$ rises in $\tau$ and $N$, $\beta$ rises in $\alpha$ and $N$, and $\psi_\tau(\beta)$ falls in $\beta$ and single-crosses from above in $\tau$, so the solution of $\psi_\tau(\beta) = 0$ falls in $N$. But the effect on equilibrium value $V$ is harder to evaluate. BMtV24 proves that $V$ rises in the degree for regular networks, $N \equiv n$, and Appendix A.5 shows the same for Poisson degrees $N \sim Pois(\lambda)$, but we do not know whether this monotonicity obtains for general, MLRP-ranked degrees $N$.

Finally, assume that agent $i$ knows her own degree $N_i = n$. Social learning $\beta = n\alpha$ scales linearly in $N_i$, so the cutoff $\tau_n$ falls in $n$ (strictly as long as $\tau_n > 0$). Contagion dynamics are still described by a one-dimensional ODE generalizing (15)

$$1 - a_t = E\left[\mathbb{I}_{\{\tau_{N'} < t\}} \exp(-\tau_{N'} - (N' - 2)\alpha_t)\right]. \tag{22}$$

But it is no longer clear how to argue equilibrium uniqueness and perform the comparative statics in Proposition 2′, since strategies are now inherently multi-dimensional, described naturally either by the cutoff vector $\{\tau_n\}_{n\geq 0}$ or the neighbor's expected experimentation $\{a_t\}_{t\geq 0}$.

# 4 Conclusion

This paper studies a simple contagion process on different kinds of configuration networks (directed, undirected, triangle) that become "tree like" for large populations. We characterize infection dynamics via simple one-dimensional ODEs and compare infection rates across networks. The model is elementary and is useful for a variety of economic applications. We illustrate this with a model of experimentation, where information spreads like an SI process.

Beyond experimentation, our results are potentially useful for a variety of economic problems where our explicit formulas can help characterize strategic behavior. For example, consider a "behavioral epidemiology" model in which agents choose to take precautions at $t = 0$ (e.g. vaccination) and interact via a contagion process (e.g. Geoffard and Philipson (1996), Kremer (1996)). Whereas our experimenting agents essentially choose the initial seeding ($\epsilon$) of the network, such precautions affect the infection rate of a link (currently

normalized to 1) or the number of neighbors from whom they can catch an infection ($N$). Alternatively, consider a model where customers become aware of a new product from other agents who purchase (e.g. Campbell (2013)). Such agents may make investments at time $t = 0$ that determine their value for the product or their degree distribution (e.g. choosing where to live).

Our directed configuration model assumes that each agent has the same number of in-, and out-stubs. This assumption ensures that the friendship paradox also arises in directed networks, which is key for the clean comparison in Proposition 2. More generally, one might consider general distributions of agents' in-, and out-stubs $(N_i^{in}, N_i^{out})$ as in the literature reviewed in Pastor-Satorras et al. (2015, chapter VII B4). Going to the opposite extreme from our assumption of perfect correlation, one might assume that agents differ ex-ante only in their out-stubs $N_i^{out}$ and that these stubs connect randomly to other agents, generating independent Poisson-distributed in-degrees. Since infection rates depend only in-degrees, the proof of Proposition 1 shows that infection rates in these networks converge to those in the associated Poisson-tree, which depends on the distribution of $N_i^{out}$ only via its expectation. Compared to our model with perfect correlation, high-degree agents (or "super-spreaders") matter only via their contribution to the average degree since they are no more likely to be infected than other agents. This difference in neighborhood structure prevents an analytical comparison with other network types as in Proposition 2.

Analogously, one could consider alternative assumptions of the connections formed by random matching. Indeed, assume that when an infected agent $i$ becomes infectious, she infects $N_i$ randomly drawn other agents $j$, instead of sampling according to their stubs $N_j$. At every instant $t$ each agent's in-degree is Poisson-distributed, but since sampling is independent across time, the time average equals the deterministic average, so infection dynamics follow $x = a = 1 - (1 - \epsilon)\exp(-E[N]\alpha)$, which is solved by Griliches (1957)'s logistic curves $a_t = x_t = 1/(1 + e^{-E[N](t+\gamma)})$. Again, high-degree agents matter only via their contribution to the average degree, marring the comparison of infection rates with networks that feature super-spreaders, Proposition 2.

# References


Bala, V., and S. Goyal (1998): "Learning from Neighbours," *Review of Economic Studies*, 65(3), 595–621.

Banerjee, A. V. (1993): "The Economics of Rumours," *Review of Economic Studies*, 107(2), 309–327.

Barthelemy, M., A. Barrat, R. Pastor-Satorras, and A. Vespignani (2004): "Velocity and Hierarchical Spread of Epidemic Outbreaks in Scale-Free Networks," *Physical Review Letters*, 92(17), 178701 1–4.

Bass, F. M. (1969): "A New Product Growth for Model Consumer Durables," *Management Science*, 15(5), 215–227.

Board, S., and M. Meyer-ter-Vehn (2021): "Learning Dynamics in Social Networks," *Econometrica*, 89(6), 2601–2635.

——— (2024): "Experimentation in Networks," *American Economic Review*, tbd(tbd), tbd.

Bonatti, A., and J. Hörner (2011): "Collaborating," *American Economic Review*, 101, 632–663.

——— (2017): "Learning to Disagree in a Game of Experimentation," *Journal of Economic Theory*, 169, 234–269.

Campbell, A. (2013): "Word-of-Mouth Communication and Percolation in Social Networks," *American Economic Review*, 103(6), 2466–98.

Decreusefond, L., J.-S. Dhersin, P. Moyal, and V. C. Tran (2012): "Large Graph Limit for an SIR Process in Random Network with Heterogeneous Connectivity," *The Annals of Applied Probability*, 22(2), 541–575.

Geoffard, P.-Y., and T. Philipson (1996): "Rational Epidemics and their Public Control," *International economic review*, pp. 603–624.

Graham, B. S. (2017): "An Econometric Model of Network Formation with Degree Heterogeneity," *Econometrica*, 85(4), 1033–1063.

Griliches, Z. (1957): "Hybrid Corn: An Exploration in the Economics of Technological Change," *Econometrica*, pp. 501–522.

Jackson, M. O. (2010): *Social and Economic Networks*. Princeton University Press.

Janson, S., M. Luczak, and P. Winridge (2014): "Law of large numbers for the SIR epidemic on a random graph with given degrees," .

Keller, G., S. Rady, and M. Cripps (2005): "Strategic Experimentation with Exponential Bandits," *Econometrica*, 73(1), 39–68.

Kiss, I., J. Miller, and P. Simon (2017): *Mathematics of Epidemics on Networks*. Springer Interdisciplinary Applied Mathematics.

Kremer, M. (1996): "Integrating Behavioral Choice into Epidemiological Models of AIDS," *Quarterly Journal of Economics*, 111(2), 549–573.

Melnik, S., A. Hackett, M. A. Porter, P. J. Mucha, and J. P. Gleeson (2011): "The Unreasonable Effectiveness of Tree-Based Theory for Networks with Clustering," *Physical Review E*, 83, 036112–1–12.

Miller, J. C. (2009): "Spread of infectious disease through clustered populations," *Journal of the Royal Society Interface*, 6, 1121–1134.

——— (2011): "A note on a paper by Erik Volz: SIR dynamics," *Mathematical Biology*, 62, 349–358.

Newman, M. (2018): *Networks*. Oxford University Press.

Niu, S.-C. (2002): "A Stochastic Formulation of the Bass Model of New-Product Diffusion," *Mathematical Problems in Engineering*, 8(3), 249–263.

Pastor-Satorras, R., C. Castellano, P. Van Miegem, and A. Vespignani (2015): "Epidemic processes in complex networks," *Review of Modern Physics*, 87, 925–979.

Ritchie, M., L. Berthouze, and I. Z. Kiss (2016): "Beyond clustering: mean-field dynamics on networks with arbitrary subgraph composition," *Mathematical Biology*, 72, 255–281.

Sadler, E. (2020): "Diffusion Games," *American Economic Review*, 110(1), 225–270.

Volz, E. (2008): "SIR dynamics in random networks with heterogeneous connectivity," *Mathematical Biology*, 56, 293–310.

Volz, E., J. C. Miller, A. Galvani, and L. A. Meyers (2011): "Effects of Heterogeneous and Clustered Contact Patterns on Infectious Disease Dynamics," *PLoS Computational Biology*, 7(6).

# A Appendix: Proofs

## A.1 Proof of Proposition 1 (Convergence SI)

We lead with the proof of part (a) for undirected networks, dropping the "upper bar", say on $\bar{a}_t$, to ease notation. Subsequently, we discuss how to adapt the proof for directed and triangular networks in parts (b) and (c) of Proposition 1.

Fix an agent $i$, a time $t \geq 0$, and an integer $r \in \mathbb{N}$, and consider "$i$'s $r$-neighborhood" $G_i^{I,r}$, that is the subnetwork of $G^I$ consisting of all agents with distance at most $r$ from the root $i$. Sadler (2020, Lemma 1) shows that for any $r$, $G_i^{I,r}$ is coupled to a branching process with offspring distribution $N$ in the first generation, and $N'-1$ in generations $2, ..., r$ with probability $1-\epsilon^{I,r}$ where $\lim_{I\to\infty} \epsilon^{I,r} = 0$. In simpler words, as $I \to \infty$, $i$ has $N$ neighbors, $N(N'-1)$ second neighbors, ..., and $N(N'-1)^{r-1}$ $r$-th neighbors, and all these neighbors are distinct.

We next define upper and lower bounds for neighbor $j$'s conditional infection rates $a_t, a_t^I$. Specifically, write $\underline{a}_t^{I,r}$ (resp. $\bar{a}_t^{I,r}$) for the expected rate conditional on no infections outside $G_i^{I,r}$ (resp. all agents outside $G_i^{I,r}$ being infected) at $t=0$; clearly, $a_t^I \in [\underline{a}_t^{I,r}, \bar{a}_t^{I,r}]$. Similarly, define the respective bounds in the infinite tree network, $a_t \in [\underline{a}_t^r, \bar{a}_t^r]$. The coupling bounds the distance between the lower bounds and the upper bounds $|\underline{a}_t^r - \underline{a}_t^{I,r}|, |\bar{a}_t^r - \bar{a}_t^{I,r}| \leq \epsilon_t^{I,r}$.[17] Below we show

$$\lim_{r\to\infty} |\bar{a}_t^r - \underline{a}_t^r| = 0. \tag{23}$$

Then, for any $I$ and $r$, by the triangle inequality

$$|a_t^I - a_t| \leq \max\{|\underline{a}_t^r - \underline{a}_t^{I,r}|, |\bar{a}_t^r - \bar{a}_t^{I,r}|\} + |\bar{a}_t^r - \underline{a}_t^r| \leq \epsilon_t^{I,r} + |\bar{a}_t^r - \underline{a}_t^r|$$

which disappears in the double-limit $\lim_{r\to\infty}\lim_{I\to\infty}$.

*Proof of (23)*: We proceed by induction over $r$. For $r=1$, this means $\underline{a}_t^1 \equiv 0, \bar{a}_t^1 \equiv 1$. More generally, writing $\underline{E}^r$ for the expectation underlying $\underline{a}_t^r$ and $\underline{\alpha}_t^r = \int_0^t \underline{a}_u^r du$ for the cumulative,

$$1-\underline{a}_t^r = \frac{\underline{E}^r[S_{j,t}S_{i,t}]}{\underline{E}^r[S_{i,t}]} = \frac{(1-\epsilon)^2 E\left[\exp\left(-(N'-1)\underline{\alpha}_t^{r-1} - (N-1)\underline{\alpha}_t^r\right)\right]}{(1-\epsilon)E\left[\exp\left(-N\underline{\alpha}_t^r\right)\right]} = (1-\epsilon)\exp\left(-(N'-1)\underline{\alpha}_t^{r-1} + \underline{\alpha}_t^r\right) \tag{24}$$

In the denominator, $i$ remains susceptible at time-$t$ if none of her $N$ neighbors infected her,

[17] These error bounds follow by definition for unconditional infection rates $s_t = E[S_{i,t}], s_t^I = E[S_{i,t}^I]$ and their associated bounds $|\underline{s}_t^r - \underline{s}_t^{I,r}|, |\bar{s}_t^r - \bar{s}_t^{I,r}| \leq \epsilon_t^{I,r}$. To confirm rigorously that the conditionial expectation in $a$ in "passes through the coupling", one would need to unpack $1-a_t = \frac{E[S_{j,t}S_{i,t}]}{E[S_{i,t}]}$ and show (23) separately for the bounds on the numerator and the denominator (and lower-bound $E[S_{i,t}] > 0$).

much as in (2). In the numerator, $i, j$ jointly remain susceptible at time-$t$ if neither has been infected by a neighbor other than each other, noting that $j$'s $N'-1$ neighbors other than $i$ are at distance $r-1$ from the boundary of $G_i^{I,r}$.

The monotonicity of (24) together with $\underline{a}_t^1 \equiv 0$ implies that $\underline{a}_t^r$ increases in $r$ and so converges to some $\underline{a}_t^\infty$ which must then solve (3), so $\underline{a}_t^\infty = a_t$ for all $t$. Similarly, $\bar{a}_t^r$ converges to $a_t$ from above, implying (23).

Convergence of unconditional infection rates $s_t^I \to s_t$ follows from (2) and their analogous bounds.

*Proof of parts (b) and (c).* The only difference is the number of neighbors in (24). For the directed network, $i$'s $r$-neighborhood $G_i^{I,r}$ is coupled to a branching process with offspring distribution $N$ in the first generation, and $N'$ in generations $2, ..., r$ since $i$'s neighbor $j$ no longer wastes one of his $N'$ outlinks to link back to $i$. (24) becomes

$$1 - \underline{a}_t^r = (1-\epsilon) E\left[\exp\left(-N' \underline{\alpha}_t^{r-1} + \underline{\alpha}_t^r\right)\right], \tag{25}$$

so as $r \to \infty$, we obtain (4).

For triangular networks, $i$'s neighbor $j$ shares one more, triangular neighbor $j'$ with $i$, as well as $N'-2$ other neighbors $k$ with distance two from $i$. Thus, (24) becomes

$$1 - \underline{a}_t^r = \frac{\underline{E}^r[S_{j,t} S_{i,t}]}{\underline{E}^r[S_{i,t}]} = \frac{E\left[\exp\left(-(N'-2)\underline{\alpha}_t^{r-1} - (N-1)\underline{\alpha}_t^r\right)\right]}{E\left[\exp\left(-N\underline{\alpha}_t^r\right)\right]} = E\left[\exp\left(-(N'-2)\underline{\alpha}_t^{r-1} + \underline{\alpha}_t^r\right)\right],$$

accounting for $j$'s $N'-2$ neighbors other than $i, j'$, and $i$'s $N-1$ neighbors other than $j$. As $r \to \infty$, we obtain (17).

## A.2 Proof of Proposition 1′ (Convergence Exp)

Just as in the proof of Proposition 1, we focus on undirected networks and drop the associated "upper bar"-notation. The neighbor's conditional infection rate $a_t^I = E[X_{j,t}^I | S_{i,t}^I]$ converges to the solution $a_t$ of (15) for any fixed cutoff $\tau$. In fact, since $a_t$ and the associated bounds $\underline{a}_t^r, \bar{a}_t^r$ rise in $\tau$ and $a_t$ is Lipschitz in $\tau$,[18] the convergence in (23) and hence of $a_t^I \to a_t$ is

[18]Indeed, at the cutoff $\frac{\partial a_t(\tau)}{\partial \tau}|_{t=\tau} = E[N_j - 1 | S_{i,\tau}, S_{j,\tau} = 0] < E[N']$. After the cutoff, we have

$$\begin{aligned}\left|\frac{\partial a_t(\tau)}{\partial \tau}\right| &= \left|\frac{\partial a_t(\tau)}{\partial \tau}|_{t=\tau} \frac{\partial a_t(\tau)}{\partial a_\tau(\tau)} - \frac{\partial a_t(\tau)}{\partial t}\right| \\ &= \frac{\partial a_t(\tau)}{\partial \tau}|_{t=\tau} \exp \int_\tau^t E[N_j - 2 | S_{j,u}, S_{i,u} = 1](1 - 2a_u(\tau)) du + \left|\frac{\partial a_t(\tau)}{\partial t}\right| < E[N'] \exp(E[N']t) + E[N']\end{aligned}$$

uniform in $\tau \in [0, \bar{\tau}]$. This implies uniform convergence of infection rates $s_t^I := E[X_t^I]$ to $s_t := E[\exp(-\tau - N\alpha_t)]$ and social learning curves $\beta_t^I := -\tau - \log s_t^I$ to $\beta_t = -\log E[\exp(-N\alpha_t)]$. For the latter, we make explicit the dependence on the cutoff and the uniform convergence

$$\lim_{I\to\infty} \sup_{\tau\in[0,\bar{\tau}]} |\beta_t(\tau) - \beta_t^I(\tau)| = 0 \tag{26}$$

We now turn to the main part of the proof of Proposition 1′, that equilibrium cutoffs and social learning curves in the finite networks $\tau^I, \beta^I$, that solve $\psi_{\tau^I}(\beta^I) = 0$ and $\beta_t^I = \beta_t^I(\tau^I)$, converge to those in the infinite tree $\tau^*, \beta^*$, that solve $\psi_{\tau^*}(\beta^*) = 0$ and $\beta_t^* = \beta_t^*(\tau^*)$, using an asterisk to distinguish $\tau^*, \beta^*$ from generic cutoffs and learning curves $\tau, \beta$. We restrict attention to a subsequence where $\tau^I$ converges to some $\tau^\infty$. The triangle inequality implies that for all $I$

$$\begin{aligned}|\psi_{\tau^\infty}(\beta(\tau^\infty))| \leq &|\psi_{\tau^\infty}(\beta(\tau^\infty)) - \psi_{\tau^\infty}(\beta(\tau^I))| + \\ &|\psi_{\tau^\infty}(\beta(\tau^I)) - \psi_{\tau^\infty}(\beta^I(\tau^I))| + \\ &|\psi_{\tau^\infty}(\beta^I(\tau^I)) - \psi_{\tau^I}(\beta^I(\tau^I))| + |\psi_{\tau^I}(\beta^I(\tau^I))|\end{aligned}$$

As $I \to \infty$, the first term vanishes by continuity of $\beta_t(\tau)$ in $\tau$, and continuity of $\psi_{\tau^\infty}(\beta)$ in $\beta = \{\beta_t\}$. The second term vanishes by continuity of $\psi_{\tau^\infty}(\beta)$ in $\beta = \{\beta_t\}$ and by (26). The third term vanishes by Board and Meyer-ter-Vehn (2024, Lemma 6(b)). The fourth term is zero for all $I$ since $\tau^I$ is the equilibrium cutoff of the $I$-agent network.

Thus, $\psi_{\tau^\infty}(\beta(\tau^\infty)) = 0$. Since $\tau^*$ is the unique solution of this equation by Lemma 1, we have $\tau^\infty = \tau^*$. Since the subsequence of $\tau^I$ that converges to $\tau^\infty$ was arbitrary, the entire sequence $\tau^I$ converges to $\tau^*$ as desired. Thus, using (26) and convergence $\tau^I \to \tau^*$ together with continuity of $\beta_t(\tau)$ in $\tau$, we get for all $t$ that

$$|\beta_t^I - \beta_t^*| = |\beta_t^I(\tau^I) - \beta_t(\tau^*)| \leq |\beta_t^I(\tau^I) - \beta_t(\tau^I)| + |\beta_t(\tau^I) - \beta_t(\tau^*)| \to 0.$$

## A.3 Proof of Proposition 3

A bit more strongly than the statement of Proposition 3, we show that "$N_1$ dominates $N_2$", i.e. $x_{1,t} > x_{2,t}$ for any $\epsilon_1, \epsilon_2 \in (0,1)$ and large enough $t$, iff $\underline{N_1} > \max\{1, \underline{N_2}\}$. For ease of

where the exponential expression for $\frac{\partial a_t(\tau)}{\partial a_\tau(\tau)}$ follows from differentiating the solution of the ODE $\dot{a} = E[N_j - 2|S_j, S_i = 1]a(1-a)$ at $t$ wrt its initial condition at $t = \tau$.

reference, we recall equations (2) and (3) for conditional and unconditional infection rates

$$x = 1 - (1-\epsilon)E[\exp(-N\alpha)]$$
$$a = 1 - (1-\epsilon)E[\exp(-(N'-2)\alpha)]$$

*Claim:* We first note that eventually everybody gets infected $x_t \to 1$ iff $\underline{N} \geq 2$.
*Proof of Claim:* If $\underline{N} \geq 2$ then $a_t \geq \epsilon$, so $\alpha_t \geq t\epsilon \to \infty$ and hence $x_t \to \infty$. If $\underline{N} = 0$, then $x_t \leq 1 - (1-\epsilon)\Pr(N=0) < 1$. If $\underline{N} = 1$, the aggregate $\alpha_t$ must be upper-bounded to avoid $a_t < 0$. This again upper-bounds $x_t$.

The claim implies that $\underline{N_1} > 1$ is necessary for $N_1$ to dominate $N_2$. It is also sufficient when $\underline{N_2} < 2$, so assume $\underline{N_1}, \underline{N_2} \geq 2$ from now. The claim also implies that

$$\frac{d}{dt}\log\frac{a}{1-a} = \frac{E[(N'-2)\exp(-(N'-2)\alpha)]}{E[\exp(-(N'-2)\alpha)]}$$

converges (exponentially) to $\underline{N} - 2$; thus $\underline{N_1} > \underline{N_2}$ is necessary and sufficient to secure $\log\frac{a_{1,t}}{1-a_{1,t}} > \log\frac{a_{2,t}}{1-a_{2,t}}$ and so $a_{1,t} > a_{2,t}$ for any base rates $\epsilon_1, \epsilon_2 \in (0,1)$ and large enough $t > 0$.

Turning to unconditional infection rates $x$

$$\frac{d}{dt}\log\frac{1}{1-x} = \frac{\dot{x}}{1-x} = \frac{E[N\exp(-N\alpha)]}{E[\exp(-N\alpha)]}a$$

converges exponentially to $\underline{N}\lim a_t$; by monotonicity of $x \to \log\frac{1}{1-x}$, $N_1$ dominates $N_2$ iff $\underline{N_1} > \underline{N_2}$.

## A.4 Proof of Proposition 2′: Welfare Ranking in (21)

We first show the comparisons between random matching and directed trees $\vec{V}^{(n+1)} > \tilde{V}^{(n)}$. We already know that $\vec{\tau}^{(n+1)} < \tilde{\tau}^{(n)}$ and now show more strongly that

$$\vec{\tau}^{(n+1)} < \tau' := \frac{n+1}{n+2}\tilde{\tau}^{(n)} \tag{27}$$

for then,

$$\vec{V}^{(n+1)} = \mathcal{V}(\vec{\tau}^{(n+1)}, (n+2)\vec{\tau}^{(n+1)} - \vec{\tau}^{(n+1)}) > \mathcal{V}(\vec{\tau}^{(n+1)}, (n+1)\tilde{\tau}^{(n)} - \vec{\tau}^{(n+1)}) > \mathcal{V}(\tilde{\tau}^{(n)}, n\tilde{\tau}^{(n)}) = \tilde{V}^{(n)},$$

where the first inequality uses (27), and the second $\tilde{\tau}^{(n)} - \vec{\tau}^{(n+1)} > 0$ and $\partial_\tau \mathcal{V} < \partial_\beta \mathcal{V} < 0$.

To see (27), we compare a neighbor's expected experimentation $\delta \geq 0$ after the cutoff for the $n$-random matching with equilibrium cutoff $\tilde{\tau}^{(n)}$, $\tilde{a}_\delta := \tilde{a}^{(n)}_{\tilde{\tau}^{(n)}+\delta}(\tilde{\tau}^{(n)})$, and the directed

$(n+1)$-tree with non-equilibrium cutoff $\tau'$ from (27), $\vec{a}'_\delta := \vec{a}^{(n+1)}_{\tau'+\delta}(\tau')$. We will show that

$$n\tilde{a}_\delta < (n+1)\vec{a}'_\delta. \tag{28}$$

Since pre-cutoff learning coincides by (27), so do cutoff beliefs $\tilde{p}^{(n)}_{\tilde{\tau}^{(n)}} = \vec{p}^{(n+1)}_{\tau'}$, and we get

$$\begin{aligned} 0 &= \psi_{\tilde{\tau}^{(n)}}(\{n\tilde{a}^{(n)}_t(\tilde{\tau}^{(n)})\}) = \tilde{p}^{(n)}_{\tilde{\tau}^{(n)}}(x + rye^{-\int_0^\infty (r+n\tilde{a}_\delta)d\delta}) - c \\ &> \vec{p}^{(n+1)}_{\tau'}(x + rye^{-\int_0^\infty (r+(n+1)\vec{a}'_\delta)d\delta}) - c = \psi_{\tau'}(\{(n+1)\vec{a}^{(n+1)}_t(\tau')\}) \end{aligned}$$

and hence in equilibrium $\vec{\tau}^{(n+1)} < \tau'$, which is (27).

We now argue (28). We first claim a partial converse, $\vec{a}'_\delta < \tilde{a}_\delta$. This follows by $\vec{a}'_0 = 1 - \exp(-(n+1)\tau') < 1 - \exp(-(n+1)\tilde{\tau}^{(n)}) = \tilde{a}_0$ and the fact that $\vec{a}'_\delta$ and $\tilde{a}_\delta$ follow the same law-of-motion $\dot{a} = na(1-a)$ (recalling (4) and (6)) and hence can't cross. Now (28) follows for $\delta = 0$ because

$$n\tilde{a}_0 = n(1-\exp(-(n+1)\tilde{\tau}^{(n)})) < (n+1)(1-\exp(-n\tilde{\tau}^{(n)})) < (n+1)(1-\exp(-(n+1)\tau')) = (n+1)\vec{a}_0 \tag{29}$$

where the first inequality uses that $(1-\exp(-x))/x$ falls in $x$, and the second inequality that $\frac{n}{n+1}\tilde{\tau}^{(n)} < \frac{n+1}{n+2}\tilde{\tau}^{(n)} = \tau'$. We show (28) for all $\delta > 0$ by arguing that $n\tilde{a}_\delta$ cannot cross $(n+1)\vec{a}_\delta$ from below: If $n\tilde{a}_\delta = (n+1)\vec{a}'_\delta$, then (using $\tilde{a}_\delta > \vec{a}'_\delta$)

$$n\dot{\tilde{a}}_\delta = n^2\tilde{a}_\delta(1-\tilde{a}_\delta) < (n+1)n\vec{a}'_\delta(1-\vec{a}'_\delta) = (n+1)\dot{\vec{a}}'_\delta.$$

This proves (28) and thus the comparison between directed trees and random matching $\vec{V}^{(n+1)} > \tilde{V}^{(n)}$.

The comparisons between undirected and directed trees $\bar{V}^{(n+2)} > \vec{V}^{(n+1)}$ (resp. undirected and triangle trees $\hat{V}^{(n+3)} > \bar{V}^{(n+2)}$), follows analogously, arguing that incentives in the undirected $(n+2)$-tree are strictly positive at $\tau' := \frac{n+2}{n+3}\vec{\tau}^{(n)}$ (resp. triangle $(n+3)$-tree at $\tau' := \frac{n+3}{n+4}\bar{\tau}^{(n)}$) by showing that the associated neighbor experimentation probabilities satisfy $(n+1)\vec{a}_\delta < (n+2)\bar{a}'_\delta$ (resp. $(n+2)\bar{a}_\delta < (n+3)\hat{a}'_\delta$). The only change is that the analogue of (29) now uses the fact that $\frac{n}{n+1}$ is less than $\frac{n+2}{n+3}$ (resp. $\frac{n+3}{n+4}$).

## A.5 Welfare increases in $N \sim Pois(\lambda)$

Here we show that welfare increases in $N \sim Pois(\lambda)$. For Poisson degrees $N' = N+1$ we can evaluate the moment-generating function explicitly

$$E[\exp(-N\tau)] = \exp\left(-\lambda\left(1-e^{-\tau}\right)\right).$$

As discussed in the body of the paper, the equilibrium cutoff $\tau(\lambda)$ falls in $\lambda$. We now show that total pre-cutoff learning $\tau + \beta_\tau = -\log E[\exp(-(N+1)\tau)] = \tau + \lambda\left(1 - e^{-\tau}\right)$ also falls in $\lambda$; this implies that equilibrium value $\mathcal{V}(\tau, \lambda(1-e^{-\tau}))$ rises in $\lambda$.

By contradiction, assume that $\tau(\lambda) + \lambda(1 - e^{-\tau(\lambda)})$ rises in $\lambda$; since $\tau(\lambda)$ falls in $\lambda$ then $\lambda(1-e^{-\tau(\lambda)-\grave{\alpha}})$ rises in $\lambda$ for any $\grave{\alpha} > 0$. Define an alternative cumulative $\grave{\alpha}_\delta = \int_{\tau(\lambda)}^{\tau(\lambda)+\delta} a_s ds = \alpha_{\tau(\lambda)+\delta} - \tau(\lambda)$ of $a_t = a_{\tau(\lambda)+\delta}$ that starts to cumulate at $\tau(\lambda)$ instead of 0. The ODE

$$\dot{\grave{\alpha}} = 1 - E\left[\exp\left(-N\tau(\lambda) - (N-1)\grave{\alpha}\right)\right] = 1 - \exp\left(\grave{\alpha} - \lambda\left(1 - e^{-\tau(\lambda)-\grave{\alpha}}\right)\right) =: \bar{h}(\grave{\alpha}; \lambda) \quad (30)$$

satisfies $\partial_\lambda \bar{h} > 0$, so its solution $\grave{\alpha}_\delta$ rises in $\lambda$. Since $\beta_{\tau+\delta} = -\log E\left[\exp\left(-N\alpha_\delta\right)\right] = \lambda\left(1 - e^{-\tau(\lambda)-\grave{\alpha}_\delta}\right)$, we get $\beta_{\tau(\lambda)+\delta}(\lambda) - \beta_{\tau(\lambda)}(\lambda) = \lambda e^{-\tau(\lambda)}\left(1 - e^{-\grave{\alpha}_\delta(\lambda)}\right)$ which rises in $\lambda$.

This leads to the contradiction that $\psi_{\tau(\lambda)}(\beta(\lambda)) = p_{\tau(\lambda)}(x + ry\int_0^\infty \exp(-r\delta - (\beta_{\tau+\delta}(\lambda) - \beta_\tau(\lambda)))d\delta)$ falls in $\lambda$, which contradicts $\psi_\tau \equiv 0$. Thus, $\tau(\lambda) + \lambda\left(1 - e^{-\tau(\lambda)}\right)$ falls in $\lambda$, as required.